

RESEARCH ARTICLE | FEBRUARY 24 2005

Optimal energy resolution of a hemispherical analyzer with virtual entry ✓

T. J. M. Zouros; E. P. Benis

*Appl. Phys. Lett.* 86, 094105 (2005)<https://doi.org/10.1063/1.1871339>View
OnlineExport
Citation

CrossMark

Articles You May Be Interested In

Charged particle trajectories in an ideal paracentric hemispherical deflection analyzer

AIP Conference Proceedings (July 2001)

Experimental energy resolution of a paracentric hemispherical deflector analyzer for different entry positions and bias

Rev. Sci. Instrum. (April 2013)

Experimental study of the polymorphism of water. II. The isobaric transitions between HDA and VHDA at intermediate and high pressures

J. Chem. Phys. (March 2018)**500 kHz or 8.5 GHz?**
And all the ranges in between.

Lock-in Amplifiers for your periodic signal measurements



Find out more



Optimal energy resolution of a hemispherical analyzer with virtual entry

T. J. M. Zouros^{a)}

Department of Physics, University of Crete, P.O. Box 2208, 71003 Heraklion, Crete, Greece
and Institute of Electronic Structure and Laser, P.O. Box 1527, 71110 Heraklion, Crete, Greece

E. P. Benis^{b)}

Department of Physics, J. R. Macdonald Laboratory, Kansas State University, Manhattan,
Kansas 66506-2604

(Received 7 July 2004; accepted 21 January 2005; published online 24 February 2005)

For an ideal hemispherical deflector analyzer (HDA) utilizing a *virtual* entry aperture whose size is controlled by an injection lens, the “slit” and angular contributions to the overall base resolution \mathfrak{R}_B are not independent, but constrained by the Helmholtz–Lagrange law. Thus, \mathfrak{R}_B becomes a function of the linear lens magnification $|M_L|$ and has a minimum, $\mathfrak{R}_{B_o} \equiv \mathfrak{R}_B(|M_L|_o)$, at the optimal magnification $|M_L| = |M_L|_o$. \mathfrak{R}_{B_o} and $|M_L|_o$ are shown to be analytic expressions of basic experimental parameters. \mathfrak{R}_{B_o} is thus the *ultimate* resolution that can be attained in this case. The generality and simplicity of this result should be very helpful in the efficient design and performance evaluation of any modern HDA. © 2005 American Institute of Physics. [DOI: 10.1063/1.1871339]

High resolution electron spectroscopy is a technique utilized in many different fields of physics, material science, chemistry, and even medicine. One of the most popular spectrometers in use is the hemispherical deflector analyzer (HDA) also available commercially from many different high tech companies. Current, modern HDAs are equipped with state-of-the art multielement zoom lens and position sensitive detector (PSD)^{1–5} [as for example in electron spectroscopy for chemical analysis (ESCA)] and therefore enjoy a very large collection efficiency. The zoom lens focuses the source electrons into the HDA entry, thus increasing the overall collection solid angle. Preretardation, also supplied by the lens, may be used to further improve the overall energy resolution of the entire spectrometer by decelerating the particles from an initial source energy T down to a much lower energy t just prior to HDA entry. In the past, when high resolution HDAs had a much lower throughput (no PSD) emphasis was primarily given to the optimization of the resolution⁶ for highest étendue^{7,8} or highest transmitted current.^{9,10} However, today, with the existing high throughput of modern ESCA spectrometers, high resolution has become of the outmost importance.

Here, we present a simple and general method for obtaining the theoretical ultimate resolution and associated linear lens magnification of a combined lens-HDA spectrometer. Our results are practical as they are analytic, giving the minimum resolution at the optimal magnification, in terms of basic experimental parameters.

The base energy resolution \mathcal{R}_B of an HDA is well known to be given by:^{6,11,14,15}

$$\mathcal{R}_B \equiv \frac{\Delta t_B}{t} = \frac{\Delta r_0 + \Delta r_\pi}{L} + \alpha_m^{*2}, \quad (1)$$

where Δr_π and Δr_0 are the exit and entry slit widths, respectively, while L is a characteristic length obtained from the HDA dispersion for nominal pass energy t . α_m^* is the maxi-

mum angle permitted by the lens-HDA geometry for the incident HDA entry angle α^* . In the case where a PSD is used instead of an exit slit, Δr_π is just the PSD position resolution. When a lens is used at the HDA entry, Δr_0 becomes the diameter of a *virtual* aperture, whose size can be adjusted by the lens' linear magnification. In this case, Δr_0 and α_m^* are *not* independent of one another but are reciprocally constrained via the Helmholtz–Lagrange law. Thus, for conjugate object-image pairs of the central ray with $T=W$ and $t=w$ and beam angle $\theta_0=0$, the Helmholtz–Lagrange law^{11,13,15} requires that:

$$|M_L| \cdot |M_\alpha| = \sqrt{F}, \quad (2)$$

with

$$F \equiv \frac{W}{w}, \quad (3)$$

$$\Delta r_0 = |M_L| d_S, \quad (4)$$

$$\alpha_m^* = |M_\alpha| \Delta \alpha_S = |M_\alpha| \left(\frac{d_p}{2l} \right), \quad (5)$$

$|M_L|$ and $|M_\alpha|$ are the absolute values of the linear and angular lens magnifications, respectively, while d_S and $\Delta \alpha_S$ are the spatial and angular extent (pencil half angle) of the particle emission at the source as shown in Fig. 1. In particular, within the paraxial approximation $\Delta \alpha_S = \frac{d_p}{2l}$, where d_p and l are the diameter of the entry pupil and its distance from the object (source) as shown in Fig. 1.

When preretardation^{6,10} is included in the overall resolution formula, L is replaced by the product $\bar{L}F$ in Eq. (1), where \bar{L} is just the mean L at $t=w$. For a conventional HDA, $\bar{L}=2\bar{R}$, where \bar{R} is just the mean HDA radius. Then, the mean source resolution $\mathfrak{R}_B \equiv \frac{\Delta T_B}{T}$ is given by:

^{a)}Electronic mail: tzouros@physics.uoc.gr

^{b)}Present address: Institute of Electronic Structure and Laser, P.O. Box 1527, 71110 Heraklion, Crete, Greece.

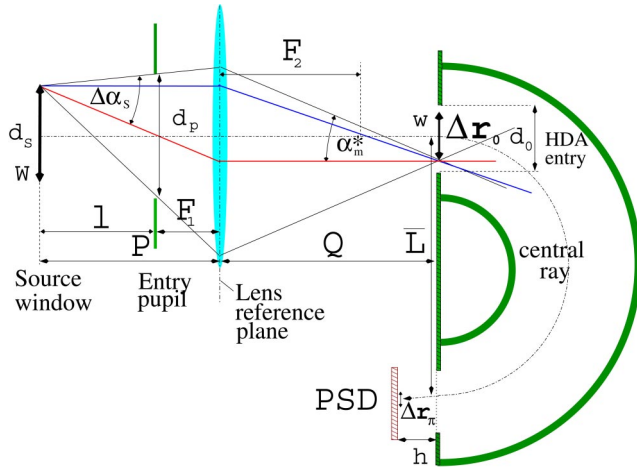


FIG. 1. (Color online) Schematic geometry of typical lens-HDA spectrometer. The object diameter d_s is focused by the lens and imaged onto the HDA entry plane as $\Delta r_0 = |M_L|d_s$. Preretardation changes the energy of the central ray from W at the source to w just prior to HDA entry. For zero beam angle (Ref. 13), the pencil half-angle $\Delta\alpha_s$, defined by the entry pupil, is related to α_m^* , via the Helmholtz-Lagrange law, $d_s\Delta\alpha_s\sqrt{W} = \Delta r_0\alpha_m^*\sqrt{w}$ [Eqs. (2)–(5)] (Refs. 11–13). The drawing has been simplified by approximating the (thick) lens by a thin lens. The vertical dimensions are particularly enhanced.

$$\overline{\mathfrak{R}_B}(|M_L|) = \frac{\overline{\mathcal{R}_B}}{F} = \frac{|M_L|d_s + \Delta r_\pi}{\bar{L}F} + \left(\frac{d_p}{2l|M_L|}\right)^2, \quad (6)$$

$\overline{\mathfrak{R}_B}$ is thus seen to be a function of $|M_L|$ and will have a minimum which can be found by setting $\partial\overline{\mathfrak{R}_B}/\partial|M_L| = 0$. This has the simple solution:

$$|M_L|_o = \left[\frac{1}{2} \left(\frac{\bar{L}F}{d_s} \right) \left(\frac{d_p}{l} \right)^2 \right]^{1/3}. \quad (7)$$

$$\overline{\mathfrak{R}_{Bo}} \equiv \overline{\mathfrak{R}_B}(|M_L|_o) = \frac{3}{2^{2/3}} \left(\frac{d_p d_s}{2l\bar{L}F} \right)^{2/3} + \frac{\Delta r_\pi}{\bar{L}F}. \quad (8)$$

As seen in Fig. 2, the minimum is most pronounced for $F=1$ and becomes increasingly more shallow for higher values of F . Both the optimal linear magnification $|M_L|_o$ and resolution $\overline{\mathfrak{R}_{Bo}}$ are seen to be functions of the source entry pa-

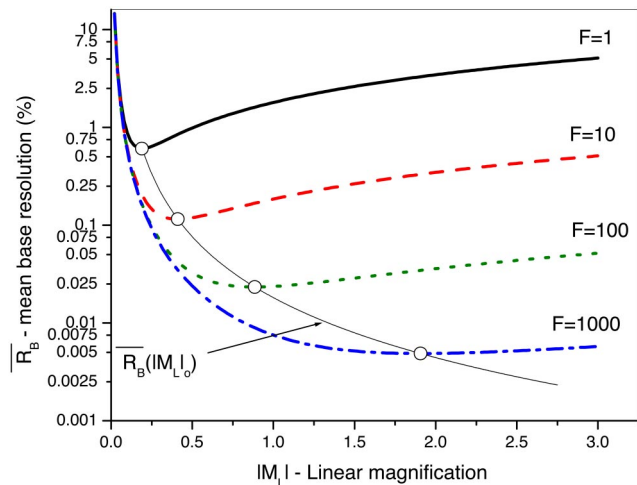


FIG. 2. (Color online) $\overline{\mathfrak{R}_B}(|M_L|)$ plotted as a function of $|M_L|$ [see Eq. (6)] for the specific spectrometer parameters listed in Table I. The position of the minima are marked with open circles. The line joining the minima is the function $\overline{\mathfrak{R}_{Bo}} \equiv \overline{\mathfrak{R}_B}(|M_L|_o)$ [see Eq. (8)].

TABLE I. List of actual spectrometer parameters ^a.

\bar{L}	151.1 mm	mean effective HDA dispersion
d_s	2.5 mm	source diameter
l	264 mm	source to entry pupil distance
d_p	4.0 mm	entry pupil diameter
Δr_π	~ 0.2 mm	PSD resolution
d_0	6.0 mm	HDA entry aperture diameter
$P+Q$	413 mm	source to image distance

^aReference 16.

rameters d_s , d_p , l (see Fig. 1), as well as the usual HDA parameters \bar{L} , F , Δr_π . This analytic dependence on d_s , d_p and l , to our knowledge, has never been presented before and should be extremely useful both in the design and performance evaluation of such a lens-HDA system. For the specific spectrometer parameters listed in Table I we have $\overline{\mathfrak{R}_{Bo}} = (1.324/F + 4.733/F^{2/3}) \times 10^{-3}$ and $|M_L|_o = 0.191F^{1/3}$ which are plotted in Fig. 3. $\overline{\mathfrak{R}_{Bo}}$ is seen to drop-off with F , while $|M_L|_o$ increases with F , ranging in values between 0.2 and 2 for $F=1-1500$. Such a broad range in the linear magnification can only be provided by a multielectrode lens.¹¹⁻¹³

When $|M_L| > d_0/d_s$, the virtual aperture size Δr_0 will exceed d_0 (the real aperture size of the HDA entry). Then, the number of particles entering the HDA will be less than those entering the lens, i.e., the transmission through the lens will drop below 100% (see Fig. 3). However, d_0 is usually much larger than Δr_0 , so an attenuation in the transmission will only occur at very high F values at which however, other limiting parameters not considered in our ideal HDA treatment could become important (e.g., external magnetic fields, aberrations etc.).

For the shape of the transmission function not to be significantly affected by the α_m^{*2} term in Eq. (1), Kuyatt and Simpson¹⁹ have proposed the following criterion for the ratio χ of the angular to the “slit” term:

$$\chi \equiv \frac{\alpha_m^{*2}}{\left(\frac{\Delta r_0 + \Delta r_\pi}{L}\right)} \leq \frac{1}{2} \quad (\text{Kuyatt-Simpson criterion}). \quad (9)$$

If the optimized values for Δr_{0o} and α_{mo}^* are used in Eq. (9),

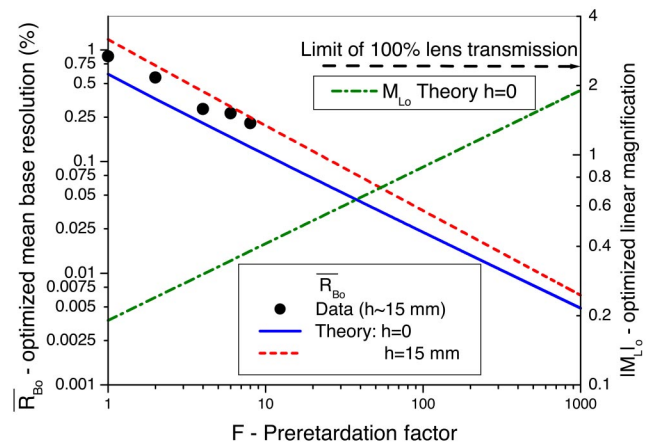


FIG. 3. (Color online) Optimized linear magnification $|M_L|_o$ (dashed-dot line and right scale) and mean base resolution $\overline{\mathfrak{R}_{Bo}}$ (continuous line and left scale) plotted as a function of F for parameters from Table I for $h=0$ and beam angle $\theta_0=0$ [see Eq. (8)]. Dashed line: $\overline{\mathfrak{R}_{Bo}}$ calculation with $h=15$ mm and $\theta_0=0$ (Ref. 17). Data: Auger electron measurements (Ref. 18).

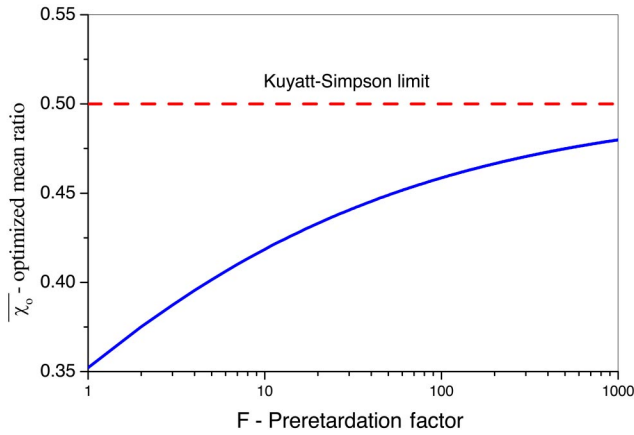


FIG. 4. (Color online) Continuous line: ratio of angular to “slit” resolution terms, $\bar{\chi}_o$, [see Eq. (10)] plotted as a function of F for the spectrometer parameters listed in Table I. Dashed line: Kuyatt-Simpson upper limit for χ [see Eq. (9)].

the mean optimized ratio $\bar{\chi}_o$ can be computed as:

$$\bar{\chi}_o = \frac{1}{2} - \left(2 + \frac{2 \left[\frac{1}{2} \left(\frac{d_s d_p}{\bar{L} F l} \right)^2 \right]^{1/3}}{\frac{\Delta r_\pi}{\bar{L} F}} \right)^{-1}, \quad (10)$$

and always fulfills the Kuyatt–Simpson criterion as seen in Fig. 4. Thus, the seemingly ad hoc value of 1/2 in the Kuyatt–Simpson criterion [Eq. (9)] is seen to arise naturally as the limit of $\bar{\chi}_o$ for $F \rightarrow \infty$. For the specific spectrometer values, $\bar{\chi}_o = \frac{1}{2} \left(1 - \frac{1}{1+2.384F^{1/3}} \right)$.

Experimental measurements of the base resolution (computed as $2 \times \text{FWHM}$), from Auger electron spectroscopy data¹⁸ taken with our spectrometer^{16,18,20} (whose basic parameters are listed in Table I) are also shown in Fig. 3 and are seen to be larger than \mathfrak{R}_{Bo} indicating that the performance of our lens+HDA has not yet been fully optimized. However, due to geometry restrictions common in such spectrometers, $h \sim 15$ mm (see Fig. 1) rather than $h=0$ as assumed in our conventional approach above. In Ref. 17 we give a more general analysis including the case where $h, \theta_0 \neq 0$. For $h=15$ mm and $\theta_0=0$, our calculations¹⁷ also included in Fig. 3 are seen to be in much better agreement with the data.

In conclusion, we have presented a simple method for obtaining the optimal base resolution of a hemispherical deflector analyzer, as well as the linear magnification of the

associated lens system under the constraints of the Helmholtz–Lagrange law for conjugate object-image pairs. The analytic results obtained can be readily used in the design and performance evaluation of such a spectrometer. Our presentation, for pedagogical reasons, has only considered the simplest possible case, in which both the beam angle θ_0 and the PSD to HDA exit plane distance h are zero. The more general problem with $h, \theta_0 \neq 0$ can also be solved in the same exact way, the results however, even though analytic, are much more cumbersome.¹⁷ Our method can in principle be extended with some modifications to include all particle spectrometers utilizing a virtual entry slit whose size is controlled by a lens and should therefore be of general interest to the spectroscopy community at large.

The authors would like to thank Professor George C. King for useful communications. This work was partially supported by the Division of Chemical Sciences, Geosciences and Biosciences, Office of Basic Energy Sciences, Office of Science, U.S. Department of Energy.

- ¹B. Wannberg and A. Sköllerö, J. Electron Spectrosc. Relat. Phenom. **10**, 45 (1977).
- ²J. E. Pollard, D. J. Trevor, Y. T. Lee, and D. A. Shirley, Rev. Sci. Instrum. **52**, 1837 (1981).
- ³P. Baltzer, B. Wannberg, and M. C. Göthe, Rev. Sci. Instrum. **62**, 643 (1991).
- ⁴P. W. Lorraine, B. D. Thoms, and W. Ho, Rev. Sci. Instrum. **63**, 1652 (1992).
- ⁵N. Mårtensson, P. Baltzer, P. A. Brühwiler, J. O. Forsell, A. Nilsson, A. Stenborg, and B. Wannberg, J. Electron Spectrosc. Relat. Phenom. **70**, 117 (1994).
- ⁶Y. Ballu, Adv. Electron. Electron Phys., Suppl. **13B**, 257 (1980).
- ⁷D. W. O. Heddle, J. Phys. E **4**, 589 (1971).
- ⁸H. D. Polaschegg, Appl. Phys. **9**, 223 (1976).
- ⁹F. H. Read, J. Comer, R. E. Imhof, J. N. H. Brunt, and E. Harting, J. Electron Spectrosc. Relat. Phenom. **4**, 293 (1974).
- ¹⁰J. C. Helmer and N. H. Weichert, Appl. Phys. Lett. **13**, 266 (1968).
- ¹¹E. Granneman and M. V. der Wiel, in *Handbook of Synchrotron Radiation*, edited by E.-E. Koch (North Holland, Amsterdam, 1983), Vol. 1A, pp. 367–456.
- ¹²D. W. O. Heddle, *Electrostatic Lens Systems*, 2nd ed. (IOP, Bristol, 2000).
- ¹³G. C. King, Exp. Methods Phys. Sci. **29A**, 189 (1995).
- ¹⁴D. Roy and D. Tremblay, Rep. Prog. Phys. **53**, 1621 (1990).
- ¹⁵J. L. Erskine, Exp. Methods Phys. Sci. **29A**, 209 (1995).
- ¹⁶T. J. M. Zouros and E. P. Benis, J. Electron Spectrosc. Relat. Phenom. **125**, 221 (2002).
- ¹⁷T. J. M. Zouros, E. P. Benis, and I. Chatzakis, Nucl. Instrum. Methods Phys. Res. B (to be published).
- ¹⁸E. P. Benis, Ph.D. dissertation, University of Crete, 2001.
- ¹⁹C. E. Kuyatt and J. A. Simpson, Rev. Sci. Instrum. **38**, 103 (1967).
- ²⁰E. P. Benis, T. J. M. Zouros, T. W. Gorczyca, A. D. González, and P. Richard, Phys. Rev. A **69**, 052718 (2004).